

Article

Influence of High-Temperature and Intense Light on the Enzymatic Antioxidant System in Ginger (*Zingiber officinale* Roscoe) Plantlets

Min Gong^{1,2}, Dongzhu Jiang^{2,3}, Ran Liu⁴, Shuming Tian^{1,2}, Haitao Xing², Zhiduan Chen⁵, Rujie Shi^{1,*} and Hong-Lei Li^{2,*}

- ¹ College of Biology and Food Engineering, Chongqing Three Gorges University, Chongqing 404100, China; gm137651@gmail.com (M.G.); shumingtian946@gmail.com (S.T.)
- ² College of Landscape Architecture and Life Science, Chongqing University of Arts and Sciences, Chongqing 402160, China; 202071714@yangtzeu.edu.cn (D.J.); xinght@cqwu.edu.cn (H.X.)
- ³ College of Horticulture and Gardening, Yangtze University, Jingzhou 433200, China
- ⁴ Chongqing Tianyuan Agricultural Technology Co., Ltd., Chongqing 402100, China; liuranfy1120@gmail.com
- ⁵ State Key Laboratory of Systematic and Evolutionary Botany, Institute of Botany, Chinese Academy of Sciences, Beijing 100093, China; zhidian@ibcas.ac.cn
- * Correspondence: 20050020@sanxiao.edu.cn (R.S.); lihonglei215@163.com (H.-L.L.)

Abstract: Environmental stressors such as high temperature and intense light have been shown to have negative effects on plant growth and productivity. To survive in such conditions, plants activate several stress response mechanisms. The synergistic effect of high-temperature and intense light stress has a significant impact on ginger, leading to reduced ginger production. Nevertheless, how ginger responds to this type of stress is not yet fully understood. In this study, we examined the phenotypic changes, malonaldehyde (MDA) content, and the response of four vital enzymes (superoxide dismutase (SOD), catalase (CAT), lipoxygenase (LOX), and nitrate reductase (NR)) in ginger plants subjected to high-temperature and intense light stress. The findings of this study indicate that ginger is vulnerable to high temperature and intense light stress. This is evident from the noticeable curling, yellowing, and wilting of ginger leaves, as well as a decrease in chlorophyll index and an increase in MDA content. Our investigation confirms that ginger plants activate multiple stress response pathways, including the SOD and CAT antioxidant defenses, and adjust their response over time by switching to different pathways. Additionally, we observe that the expression levels of genes involved in different stress response pathways, such as SOD, CAT, LOX, and NR, are differently regulated under stress conditions. These findings offer avenues to explore the stress mechanisms of ginger in response to high temperature and intense light. They also provide interesting information for the choice of genetic material to use in breeding programs for obtaining ginger genotypes capable of withstanding high temperatures and intense light stress.

Keywords: ginger; malonaldehyde (MDA); superoxide dismutase (SOD); catalase (CAT); environmental stress



Citation: Gong, M.; Jiang, D.; Liu, R.; Tian, S.; Xing, H.; Chen, Z.; Shi, R.; Li, H.-L. Influence of High-Temperature and Intense Light on the Enzymatic Antioxidant System in Ginger (*Zingiber officinale* Roscoe) Plantlets. *Metabolites* **2023**, *13*, 992. <https://doi.org/10.3390/metabo13090992>

Academic Editors: Baoguo Du, Youjun Zhang and Michał Tomczyk

Received: 12 July 2023

Revised: 31 August 2023

Accepted: 2 September 2023

Published: 4 September 2023



Copyright: © 2023 by the authors. Licensee MDPI, Basel, Switzerland. This article is an open access article distributed under the terms and conditions of the Creative Commons Attribution (CC BY) license (<https://creativecommons.org/licenses/by/4.0/>).

1. Introduction

Global warming causes frequent climate anomalies, while ecological issues pose significant challenges to agricultural production [1]. Plants are often subjected to various adverse conditions during their growth and development [2]. Temperature and light are two critical factors that impact plant yield [3,4]. High temperature (HT) can trigger the accumulation of reactive oxygen species (ROS), which possess strong oxidizing ability and can damage many biological macromolecules [5]. In normal conditions, plant cells maintain a dynamic balance between the production and elimination of intracellular ROS, which does not pose any harm to plant function [6]. Excessive HT stress can lead to the accumulation of ROS, resulting in decreased enzymatic reaction efficiency, physiological

metabolism inactivation, cell death, reduced photosynthetic rate, poor assimilate formation, and even decreased yield and fruit quality [7]. HT conditions are generally accompanied by intense light (IL); this combined stress represents one of the primary limiting factors during the life process of plants. Research has demonstrated that plants are significantly more affected by a combination of HT and IL stress rather than experiencing either HT or IL individually [8].

To combat the harmful effects of ROS, plants have developed a sophisticated antioxidative defense system that includes enzymatic and non-enzymatic antioxidants [9]. These enzymatic antioxidants include SOD, CAT, LOX, and NR [10]. These enzymes work together to scavenge ROS and neutralize them before they can damage cellular components. SOD is active in eliminating excess ROS and superoxide anions in plants [11]. CAT aids the removal of hydrogen peroxide toxicity in plants [12]. However, the action conditions of antioxidant enzymes are generally mild. Severe stress conditions can inactivate them, leading to the breakdown of the enzymatic defense system and the accumulation of hydrogen peroxide and ROS [13]. Studies demonstrate that heat-resistant rice varieties enhance heat stress tolerance by increasing antioxidant enzyme activity and reducing ROS and MDA content under HT stress conditions [14]. LOX is another vital enzyme in plants that catalyzes the production of fatty acid derivatives from phenolic glycerides [15]. This pathway is one of the most vital means of fatty acid oxidation in plants, which is typically activated under stress conditions. LOX is closely linked to plant disease and injury resistance. NR is an oxidoreductase that plays a key role in catalyzing the conversion of nitrate to nitrite [16].

Plants continuously produce ROS in response to stress conditions, resulting in the generation of malonaldehyde (MDA), as activity of antioxidant enzymes and altered levels of transcription of antioxidant enzymes [17,18]. These parameters are commonly employed as indicators of oxidative damage to cell membranes and cells, which in turn, help to assess the HT tolerance of plants [19]. Studies have demonstrated that the cold-inducible gene *RCI3* of *Arabidopsis thaliana* positively regulates salt and drought stresses [20]. Moreover, it has also been revealed that *LOX* genes exhibit differential expression in the roots, stems, leaves, flowers, fruits, and seeds of plants [21]. In tomato, for instance, the 14 *LOX* genes have different expression levels when subjected to four abiotic stresses, including heat, cold, drought, and salt [22]. The expression profile of *SOD* in foxtail millet was investigated in response to drought, salt, and cold treatments using quantitative real-time PCR (qRT-PCR) [23]. Results indicated that each *SOD* gene responded to at least one abiotic stress condition. Meanwhile, Curtis [24] reported a decline in nitrate content in lettuce leaves upon the expression of the *NR* recombinant gene. Conversely, the expression of the *NR* gene was triggered by light, carbohydrate, and NO_3^- .

Ginger (*Zingiber officinale* Roscoe) is an herbaceous perennial belonging to the genus *Zingiber* (fam. Zingiberaceae). The rhizomes possess both medicine and culinary properties. Due to its high yield per unit area and substantial economic benefits, ginger is an economically significant crop that warrants widespread cultivation [25]. *Z. officinale* is a shade-loving species [26], therefore it does not tolerate IL. The daily average temperature suitable for ginger growth is 20–28 °C [27]. Strong solar radiation is detrimental for plantlets, especially when combined with an air temperature above 35 °C [28]. Under intense sunlight, ginger plantlets grow poorly, leaf blades do not expand properly, plant forking is delayed, and the transition from vegetative growth to reproductive growth is prolonged. Additionally, the leaf color turns yellowish. Ultimately, these conditions lead to thin ginger plants, low yield, and poor quality [29]. High-temperature-induced damages to ginger have been increasingly common and severe in recent years, leading to substantial losses of production. Notably, during the summer of 2022 in Chongqing (China), prolonged extreme HT periods resulted in pronounced physiological damage to ginger, evident by the widespread effects on crop yield and quality. In July, ginger is at the plantlet stage. During this period, it grows more slowly, with the main focus on stem and root growth. However, few reports are available on the underlying response mechanism of ginger to HT and IL stresses, which subsequently hinders the progression of breeding efforts. Hence, there

appears to be an essential need to explore the unresolved response mechanisms associated with HT and IL exposure in ginger crops.

In the present study, we measured the MDA content and enzyme activity of ginger leaves after 4 consecutive days of exposure to natural HT and IL. Furthermore, we employed bioinformatics to analyze the response mechanism of *SOD*, *CAT*, *LOX*, and *NR* genes in ginger to HT and IL stress. We detected several enzyme gene family members and analyzed the various response patterns of enzyme genes under HT and IL stresses.

2. Materials and Methods

2.1. Plant Materials

Ten rhizomes of *Zingiber officinale* cv. Southwest, also known as Zhugen ginger, were transplanted into ten pots containing sterilized soil (50 cm × 21 cm × 25 cm) on 15 May 2022. Subsequently, they were cultivated in the greenhouse of the College of Landscape Architecture and Life Science, Chongqing University of Arts and Sciences. The cultivation conditions included a temperature of 25 °C, humidity of 75%, light intensity of 200 $\mu\text{E m}^{-2} \text{s}^{-1}$ [30], and a photoperiod of 14 h (from 6 am to 8 pm) of light and 10 h of darkness. The light intensity was adjusted using a sun-shading net and LEDs (BN058C LED 11/CW L1200, Signify Luminares (Shanghai) Co., Ltd. Shanghai, China). This cultivation period lasted for 60 days. Afterward, all ten ginger plantlets were moved to open-air conditions in Chongqing (29°14'21.912" N, 105°52'14.088" E), where they were exposed to natural conditions at 8 am from 14 July to 17 July. During this period, we stopped watering the ginger plantlets. The maximum temperature reached peaks above 39 °C and the light intensity reached up to 1920 $\mu\text{E m}^{-2} \text{s}^{-1}$ (Table 1). The adult leaves (the third to fifth unfolding leaves from the top) were collected at 8:30 a.m. on the first day as the control group and at 3:00 p.m. on the first, second, third, and fourth days as the test group. In order to carry out subsequent analyses, the plantlets grown in the greenhouse before being moved to open-air conditions were used as the control. Three adult leaves from three randomly selected ginger plantlets were collected, with one leaf chosen from each plant and mixed. The mixed leaves were immediately stored in liquid nitrogen for subsequent determination of enzyme activity and qRT-PCR. Three technical replicates were conducted independently to ensure accuracy and reliability of the results.

Table 1. Primer sequences used in qPCR.

Gene Name	Forward Primer (5' → 3')	Reverse Primer (5' → 3')
ZoSOD3	GTGACCTGGGAAACATCG	GCCAATCTTCCTCCAGCA
ZoSOD11	AAACAGGCGGAACACGAC	CAGTCCCTTCCCATCCAG
ZoSOD13	TTTCTGCTTCTGTGCCCAGTT	GCTGCTTCCTCGGTCAAA
ZoSOD14	GGTGTGTGCTGCTCCTGGTA	AGGGAAATCTGGCTATCAACA
ZoCAT1	GCTGCTGCGATTCTGTCT	CTTTCGGTTCTCCAGTCG
ZoCAT2	GCACCGTCTAGGACCAAAC	GCTTTCTCACGCCTTCCT
ZoCAT3	ATTCTTGACTTCTCGCACCA	CAGCAGCAATAGAATCATAAAG
ZoCAT4	GTGGGCAGGCTGGTGCTC	TGAGTCCGTCGTAGTGTTG
ZoLOX5	GCCTACGCCTACTACAACGACC	CACATAGATGTCCAGGCTTAGC
ZoLOX12	GCAAGGTGGAGATGATAACG	TCCGGCGTATCGTATCTG
ZoLOX18	CGAGGCGTTGGAGCAGAAGA	TAATGCCGTGCGAGTTGAT
ZoLOX21	GCCCTGCTGGATGAACCT	ATCGCCCCGAGTTGGACCTG
ZoNR2	TGTGAAGGTCTACACCCTGACTGAG	TCCTGGTTGTAGTGCCGTTG
ZoNR6	TCATCCACTGGGAAAGATGC	AATCTGAGGCCACAGCA
ZoNR7	TTCTGAAGTAAGTGGGCACA	CTGCCAGTTGCTCCACGA
ZoNR22	GTTCTTACGGTGCTGGCTTTG	GGTCCACCTGGTCCATAAA
ZoTUB2	GAACATGATGTGTGCTGCCG	ATCTTCAGCCCTTTCGGAGG

2.2. Evaluation of Ambient Conditions, Chlorophyll Index, and Plant Phenotypic Changes

To determine the illuminance, air temperature, and leaf temperature around the ginger plant, we employed an illuminometer (Pro'sKit, MT-4617LED-C, Prokit's Indus-

tries Co., LTD., Taiwan, China). To assess the relative chlorophyll index, we utilized a chlorophyll meter (SPAD-502 Plus/DL, Spectrum Technologies, Inc., Aurora, IL, USA). Measurements were taken on leaves from three randomly selected ginger plantlets, ensuring the accuracy and reliability of the data obtained. Plant phenotypic changes were assessed by taking photographs with a Nikon D610 camera (NIKON CORPORATION, Japan) under the following shooting conditions: aperture value: f/7.1, exposure time: 1/125 s, ISO speed: ISO-200, focal length: 28 mm.

2.3. Determination of MDA Content and Activity Assay of Enzymes

2.3.1. Determination of MDA Content

The samples were homogenized in an ice bath and the resulting extract volume was used for analysis. Subsequently, the supernatant was collected by centrifuging at $8000 \times g$ for 10 min at $4\text{ }^{\circ}\text{C}$. The content of malondialdehyde (MDA) was determined using the thiobarbituric acid (TBA) method [31]. MDA reacts with TBA, forming a red product with a maximum absorption peak at 532 nm. The colorimetry technique allows for estimation of the lipid peroxide content in the sample. Additionally, the absorbance at 600 nm was measured and the difference between the absorbance at 532 nm and 600 nm was used to calculate the MDA content. The samples were then placed on ice for testing. The determination procedure followed the MDA Colorimetric Assay Kit protocol (Chongqing Bonoheng Biotechnology Co., Ltd., Chongqing, China).

$$\text{MDA content (nmol/g FW)} = [\Delta A \times V \div (\epsilon \times d) \times 10^9] \div (W \times V1 \div V2)$$

where V is the total volume of reaction system (L), ϵ is the molar extinction coefficient of malondialdehyde (L/mol/cm), d is the optical path of cuvette (cm), V1 is the volume of added sample (L), V2 is the volume of extraction solution added (L), W is the sample quantity (g).

2.3.2. Determination of SOD Activity

The sample preparation method is the same as MDA. Superoxide anion ($\text{O}_2^{\cdot-}$) generation occurs through the xanthine and xanthine oxidase reaction system. $\text{O}_2^{\cdot-}$ can reduce nitroblue tetrazolium (NBT) to produce a blue dye, which absorbs at 560 nm. Superoxide dismutase (SOD) can scavenge $\text{O}_2^{\cdot-}$, thereby inhibiting the formation of formazan. The intensity of the blue color in the reaction solution indicates the SOD activity, with a deeper blue color indicating lower activity and a higher SOD activity. The determination procedure followed the Superoxide Dismutase (SOD) Activity Assay Kit (Chongqing Bonoheng Biotechnology Co., Ltd., Chongqing, China).

$$P = (A1 - A2) \div A1 \times 100\%$$

$$\text{SOD activity (U/g FW)} = [P \div (1 - P) \times V] \div (W \times V1 \div V2) \times N$$

where P is the inhibition percentage (U/g), A1 is the absorbance value of the control tube, A2 is the absorbance value of the experimental tube, V is the total volume of reaction (mL), V1 is the sample volume added to the reaction system (mL), V2 is the volume of extract added (mL), W is the sample quantity (g), N is the dilution factor of samples.

2.3.3. Determination of CAT Activity

The sample preparation method is the same as MDA. H_2O_2 exhibits a characteristic absorption peak at 240 nm. Catalase (CAT) is capable of decomposing H_2O_2 , leading to a decrease in absorbance of the reaction solution at 240 nm over time. The CAT activity is calculated based on the rate of change of absorbance. The determination procedure followed the Catalase (CAT) Activity Assay Kit (Chongqing Bonoheng Biotechnology Co., Ltd., Chongqing, China).

$$\text{CAT(U/g FW)} = [\Delta A \times V \div (\epsilon \times d) \times 10^9] \div (V1 \div V2 \times W) \div T$$

where V is the total volume of reaction (mL), ϵ is the H_2O_2 molar extinction coefficient, d is the optical path of cuvette (L/mol/cm), V_1 is the volume of added sample (mL), V_2 is the volume of extraction solution added (mL), T is the reaction time (min), W is the sample quantity (g), 10^9 is the unit conversion factor, 1 mol is 10^9 nmol.

2.3.4. Determination of LOX Activity

To prepare the sample for analysis, 0.1 g of the sample was weighed and 1 mL of reagent 1 was added for ice bath homogenization. The supernatant was collected by centrifugation at $16,000 \times g$ for 20 min at 4 °C. LOX catalyzed the oxidation of linoleic acid, resulting in the formation of an oxidation product with a characteristic absorption peak at 234 nm. The rate of increase in absorbance at 234 nm was measured to calculate the LOX activity. The collected sample was then placed on ice for testing. The determination procedure followed the Plant Lipoxygenase (LOX) Activity Assay Kit (Chongqing Bonoheng Biotechnology Co., Ltd., Chongqing, China).

$$\text{LOX (U/g FW)} = [(A_4 - A_3) - (A_2 - A_1)] \times V \div (W \times V_1 \div V_2) \div T \times 1000$$

where V is the total volume of reaction system (U/g), V_1 is the the supernatant volume of D that was added to the reaction system (mL), W is the sample quantity (g), V_2 is the total volume of supernatant (mL), T is the reaction time (min).

2.3.5. Determination of NR Activity

An amount of 0.1 g of the sample was weighed and 1 mL of extracting solution was added for ice bath grinding. The supernatant was collected by centrifugation at $4000 \times g$ for 10 min at 4 °C. NR catalyzed the reduction of nitrate to nitrite through the reaction: $NO_3^- + NADH + H^+ \rightarrow NO_2^- + NAD^+ + H_2O$. NADH exhibited a characteristic absorption peak at 340 nm and the change in absorbance value at 340 nm was indicative of the enzyme activity. To induce the sample, it was soaked with an inducer for 2 h. The collected sample was then placed on ice for testing. The determination procedure followed the Nitrate Reductase (NR) Activity Assay Kit (Chongqing Bonoheng Biotechnology Co., Ltd., Chongqing, China).

$$\text{NR (U/g FW)} = [\Delta A \times V \div (\epsilon \times d) \times 10^6] \div (W \div V_2 \times V_1) \div T$$

where V is the total volume of reaction system (mL), V_1 is the volume of added sample (mL), V_2 is the volume of extraction solution added (mL), T is the reaction time (min), ϵ is the molar extinction coefficient of NADH (L/mol/cm), d is the optical path of cuvette (cm), W is the sample quantity (g), 10^6 is the unit conversion factor, 1 mol is 10^6 nmol.

2.4. Analysis of Enzyme Coding Genes

In order to identify all enzyme coding genes of *SOD*, *CAT*, *LOX*, and *NR* in ginger, we downloaded the HMM model file of each enzyme gene from the Pfam database (<http://pfam-legacy.xfam.org/>, accessed on 21 December 2022). Based on the HMM file as the search criterion, we executed the Hmm search program in HMMER3.0 on the ginger genome [32]. The candidate genes were judged by using a score value of ≥ 100 and $e\text{-value} \leq e^{-10}$. To eliminate duplicates, we carried out identification and screening of protein domains via NCBI-CDD (<https://www.ncbi.nlm.nih.gov/>, accessed on 23 December 2022). As a result, we obtained the protein sequence of each ginger enzyme gene family, followed by the utilization of MEGA7.0 software to perform multiple sequence alignment of each enzyme gene family. Subsequently, the adjacent-joining (NJ) method was employed to construct the phylogenetic tree of enzyme proteins of the ginger gene family and Arabidopsis gene family with the bootstrap value set to 1000; other parameters maintained default [33].

2.5. Expression Analysis of Enzyme Coding Genes by qRT-PCR

The study utilized qRT-PCR (qTOWER 2.2, Analytik Jena AG, Germany) to assess the expression of enzyme genes under abiotic-stress conditions. To minimize experimental errors, the materials were subjected to three repeated experiments. All four ZoCAT genes were deliberately selected, while for the other three enzymes, four genes were randomly chosen. The primers for qRT-PCR were designed using Primer5 software (<http://frodo.wi.mit.edu/>, accessed on 29 December 2022) (Table 1). The ZoTUB2 gene was used as an internal control. The PCR program consisted of an initial denaturation at 95 °C for 30 s, followed by 40 cycles of 95 °C for 10 s and 60 °C for 30 s. Biological triplicates were used for each reaction. The relative expression level of each enzyme gene was calculated using the $2^{-\Delta\Delta CT}$ method [34].

2.6. Statistical Analyses

The statistical analysis was conducted with IBM SPSS Statistics 22. This involved performing a one-way analysis of variance (ANOVA) and species-specific Duncan's multiple range tests to compare the mean values of different exposure treatments to HT and IL times. Furthermore, Origin Pro 2022 version software was used to generate a column analysis chart using all individual response variable data points. This approach ensured accurate representation of the results and minimized academic plagiarism risks.

3. Results

3.1. The Changes of Chlorophyll Index under HT and IL Stress

HT and IL conditions showed significant impact on the growth of *Z. officinale* cv. Southwest, as depicted in Figure 1. With increasing time exposure to HT and IL, ginger leaves displayed prominent signs of curling, yellowing, and even withering. Air temperature, illumination, leaf temperature, and chlorophyll were measured at various time intervals, as reported in Table 2. The temperature and illumination were significantly lower in the control group compared with the experimental group during the four-day period of HT and IL stress. Initially, the chlorophyll index was approximately 29.27 SPAD (soil and plant analyzer development), but it decreased throughout the exposure to HT and IL treatment, reaching its lowest point on the fourth day at 15.9 SPAD.

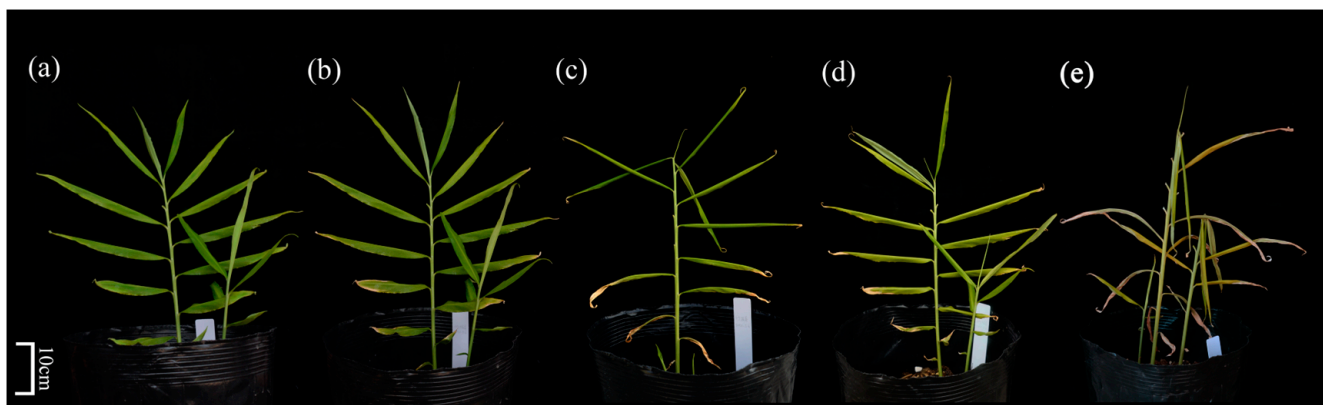


Figure 1. The phenotypic changes of *Zingiber officinale* cv. Southwest before (a) and after being exposed to HT and IL for four consecutive days (b–e).

Table 2. Ambient conditions, leaf temperature, and chlorophyll index of *Zingiber officinale* cv. Southwest under HT and IL.

Treatments	Daily Temperature Range (°C)	Average Ambient Temperature during Measurement (°C)	Leaf Temperature (°C)	Light Intensity ($\mu\text{E m}^{-2} \text{s}^{-1}$)	Chlorophyll Index (SPAD)
control	25	30.67 \pm 0.57 d	28.95 \pm 0.49 d	982.44 \pm 78.60 e	29.93 \pm 0.85 a
1d	33~41	39.00 \pm 0.26 c	34.70 \pm 0.63 b	1920.01 \pm 6.49 a	29.27 \pm 0.57 a
2d	34~40	41.23 \pm 0.40 b	33.58 \pm 0.70 c	1786.31 \pm 10.38 d	24.17 \pm 0.31 b
3d	31~39	41.30 \pm 0.75 b	35.04 \pm 0.59 ab	1792.85 \pm 16.23 c	20.53 \pm 1.25 c
4d	34~40	42.90 \pm 0.66 a	36.04 \pm 0.32 a	1810.04 \pm 9.26 b	15.90 \pm 0.55 d

PS: data shown are means \pm SD (n = 3). Different lowercase letters after the same column data indicate significant differences between different treatments ($p < 0.05$).

3.2. Malondialdehyde Contents

The MDA content was initially low in the control group but steadily increased from the first day. The highest MDA content was observed on the second day under HT and IL stress (319.00 ± 2.67 nmol/mL FW). From the third day onwards, the MDA content gradually decreased. A significant decrease was observed on the fourth day (Figure 2).

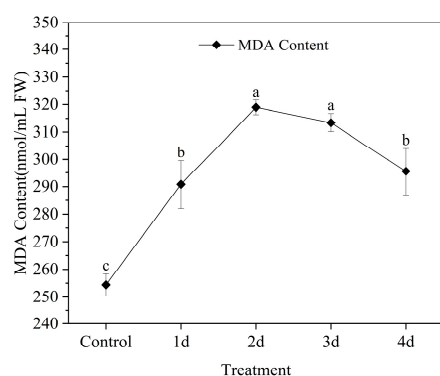


Figure 2. MDA content in leaves of *Z. officinale* under HT and IL treatment for 4 days. Data shown are means \pm SD (n = 3). Different lowercase letters in the same group of data indicate significant differences between different treatments ($p < 0.05$).

3.3. Protective Enzyme Activities

The activity of SOD exhibited a gradual increase with prolonged exposure to HT and IL. Notably, the highest SOD activity was observed on the second day under HT and IL stress, recording 374.99 ± 5.76 U/g FW (Figure 3a). However, with further exposure to the HT, the SOD activity displayed a gradual decline over time.

Comparing the CAT activity in the control group, there was a significant increase in activity observed on the first day. There was no significant change in CAT activity during the four-day HT and IL stress treatment. The highest CAT activity was observed on the third day, recording 1817.96 ± 30.00 U/g FW (Figure 3b). On the fourth day, the CAT activity slightly declined compared with the first and third day.

During the first two days of the HT and IL treatment, no significant difference in LOX activity was observed, remaining stable at approximately 22,921.74 (U/G prot). However, on the third day, the LOX activity showed a significant decrease compared with the second day. The LOX activity declined to its lowest level on the fourth day, as depicted in Figure 3c.

There was a significant reduction in the NR activity observed on the first day under HT and IL stress. The highest NR activity was recorded on the second day after undergoing the HT and IL (22.36 ± 0.41 U/g FW), while the lowest activity was observed on the third day (16.13 ± 0.33 U/g FW) (Figure 3d).

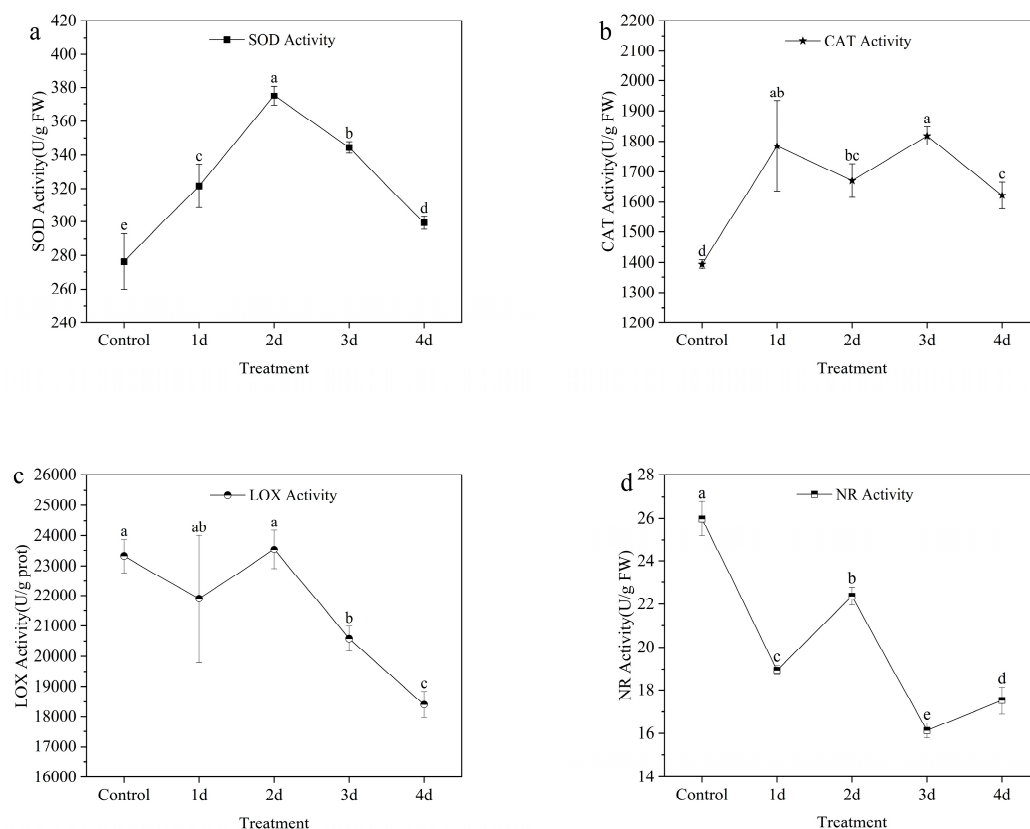


Figure 3. The activities of enzymes (SOD, CAT, LOX, and NR) (a–d) in leaves of *Z. officinale* under HT and IL for 4 days. Data shown are means \pm SD ($n = 3$). Different lowercase letters in the same group of data indicate significant differences between different treatments ($p < 0.05$).

3.4. Identification of Enzyme Coding Genes in Ginger

The HMM models of SOD domain (PF00080, PF00081, PF02777), CAT domain (PF00199), LOX domain (PF01477, PF00305), and NR domain (PF00173) were extracted from the ginger genome data using the HMMER program. Sequences with expected values E less than 10^{-5} were removed and their domain was validated with the CD search program. A total of 19 SOD gene family members (78–432 aa), 4 CAT gene (560–2348 aa) family members, 21 LOX gene family members (187–938 aa), and 28 NR gene (101–897 aa) family members were identified. These genes were designated as *ZoSOD1*–*ZoSOD19*, *ZoCAT1*–*ZoCAT4*, *ZoLOX1*–*ZoLOX21*, and *ZoNR1*–*ZoNR28* according to their positional order on the ginger protein sequence.

3.5. Phylogeny of the Enzyme Coding Genes

To analyze the phylogenetic relationships between the full-length enzyme gene sequences of *Zingiber officinale* and *Arabidopsis thaliana*, an unrooted phylogenetic tree was constructed based on their alignment. The analysis revealed that the 19 *ZoSODs* could be classified into 3 groups, while the 4 *ZoCATs* could be grouped into 2 groups (I–II). Furthermore, the 21 *ZoLOXs* were clustered into 2 groups and the 28 *ZoNRs* had robust bootstrap value support, indicating their conserved phylogenetic relationships. Based on the phylogenetic analysis, the 28 SOD proteins were classified into 3 groups, namely group I (Cu/ZnSODs), group II (Mn-SODs), and group III (Fe-SODs) (Figure 4a). The seven CAT proteins were categorized into two subfamilies, where subfamily I comprised *ZoCAT2* and *ZoCAT3*, while subfamily II contained *ZoCAT1* and *ZoCAT4* (Figure 4b). Moreover, the 27 LOX proteins could be grouped into two, 9-LOX subtype and 13-LOX subtype, consistent with the types of domains they possess (Figure 4c).

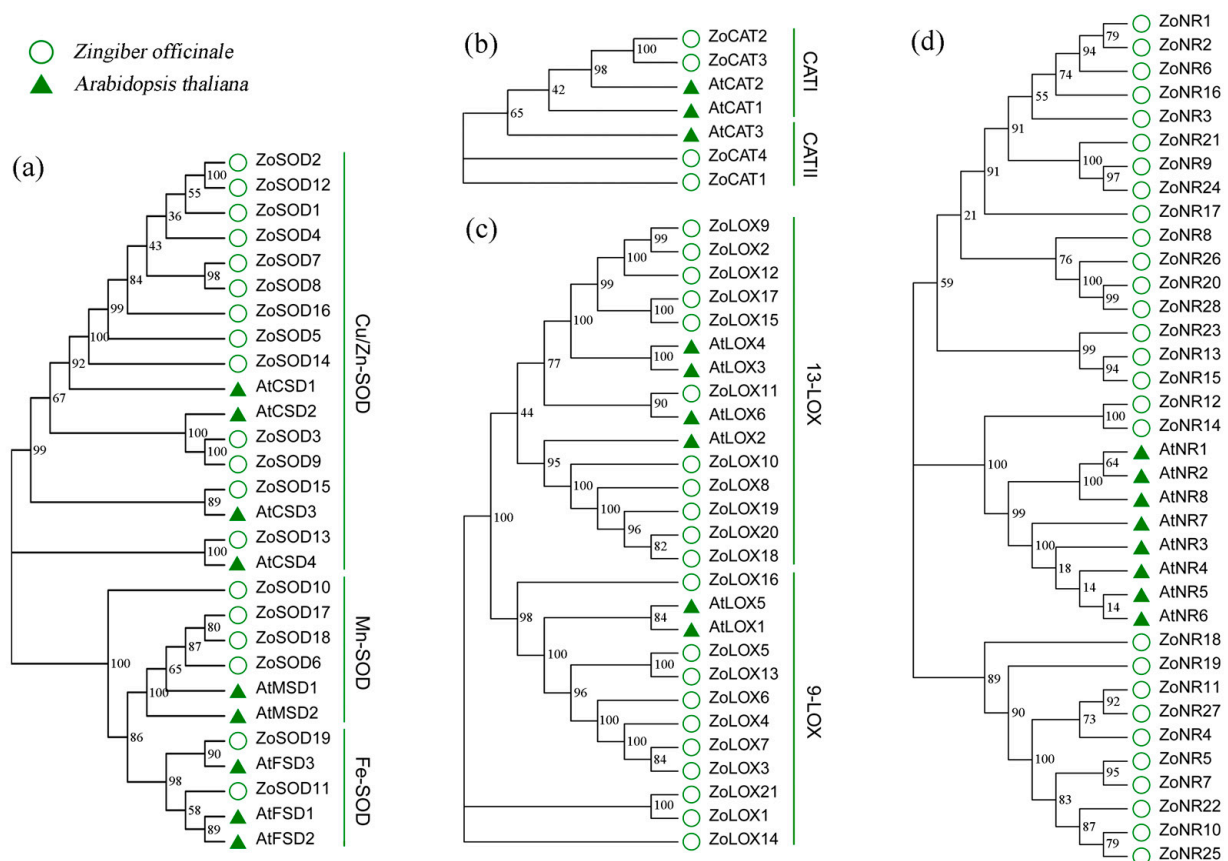


Figure 4. A phylogenetic analysis of enzyme gene families in *Z. officinale*. (a) SOD family, (b) CAT family, (c) LOX family, and (d) NR family. The round shapes represent the enzyme gene family members of *Z. officinale*, while the triangle shapes represent those of *Arabidopsis thaliana*.

3.6. Expression Pattern of Enzyme Genes

To investigate the involvement of enzyme gene families in adversity, q RT-PCR was employed to analyze the expression of enzyme genes under HT and IL. The results depicted in Figure 5 demonstrated that various enzyme genes displayed different expression patterns under HT and IL stress. On the initial day of HT and IL treatment, there was a notable upregulation in the expression of antioxidant reductase genes such as SOD and CAT, along with a significant downregulation of the oxidoreductase gene LOX, which corresponded with the changes observed in enzyme activity. ZoSOD11, ZoSOD13, and ZoSOD14 exhibited evident upregulation under stress initially, followed by a gradual decrease. The expressions of ZoCAT1, ZoCAT3, and ZoCAT4 genes were upregulated. However, ZoCAT2 displayed a significant downregulation from the initial day. The gene expressions of ZoLOX5, ZoLOX12, and ZoLOX18 also showed a significant downward trend, with ZoLOX21 exhibiting a consistent high level of expression. In contrast, the expressions of ZoNR2, ZoNR6, and ZoNR22 genes were initially upregulated on the second day but later downregulated. Conversely, ZoNR7 showed significant upregulation from the first day and maintained a high level of expression.

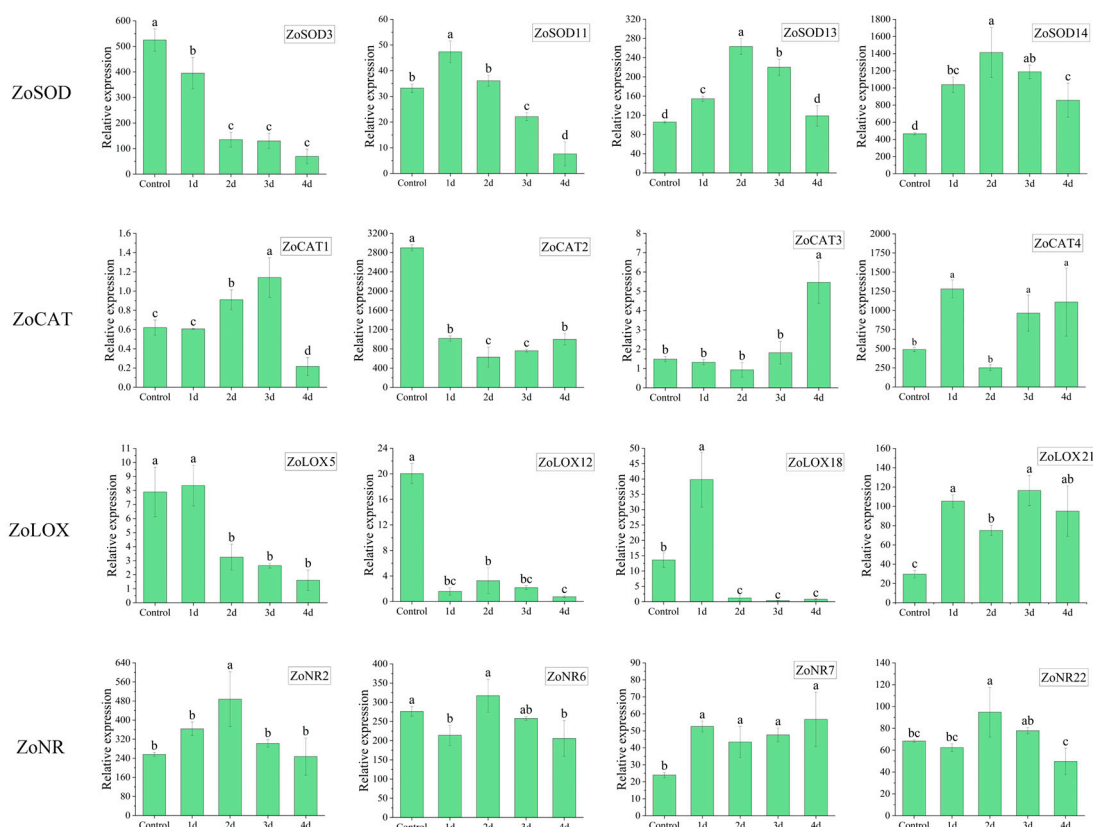


Figure 5. Relative expression of enzyme genes in ginger leaves under HT and IL stress. Data shown are means \pm SD ($n = 3$). Different lowercase letters in the same group of data indicate significant differences between different treatments ($p < 0.05$).

4. Discussion

The present study demonstrated that *Z. officinale* cv. Southwest is sensitive to HT and IL conditions. This was evidenced by the significant reduction in the chlorophyll index and the increase in MDA content, a marker of oxidative stress, in response to HT and IL stress treatment. These results are consistent with those of previous research indicating that HT and IL stress can cause oxidative damage to plant cells, leading to a decrease in chlorophyll index and an increase in MDA content [35]. The subsequent decrease in MDA may have resulted from the damage caused by continuous high-temperature stress to the intracellular membrane system of ginger cells [36].

In recent years, some research reports have suggested that SOD can protect plants from abiotic and biotic stress, such as heat, cold, drought, and salinity [37,38]. We observed a consistent increase in SOD activity on the first day of HT and IL stress treatment, suggesting the activation of an antioxidant response system in ginger plants. A similar response was also reported in other plant species, such as mung bean (*Vigna radiata* (L.) R. Wilczek), wheat (*Triticum aestivum* L.), and tomato (*Solanum lycopersicum* L.), which also showed an increase in SOD activity under HT stress [39,40]. The increase in SOD activity could be attributed to the excessive production of superoxide radicals that are toxic to cells, making defense against oxidative stress important for plant cells. Under various environmental stress conditions, researchers have found that different types of SOD genes have different expression patterns. Under stress conditions, SOD genes in *Arabidopsis* show different degrees of differential expression; *FSD1* is a gene that shows significantly increased expression under heat stress [41]. *ZoSOD11* is a direct homologous gene of *AtFSD1* and it shows significant differential expression in ginger under HT and IL stress. In addition, the expression patterns of *ZoSOD13* and *ZoSOD14* are similar to that of *ZoSOD11*, indicating that the function of these genes is related to HT and IL stress. On the other hand, SOD3 and

other genes are not significantly expressed under stress. This is consistent with previous research, such as in *Arabidopsis*, where the expression of *MnSOD* did not change under oxidative stress conditions, but researchers found that *MnSOD* expression significantly changed under drought stress in wheat and cotton [42,43]. On the second day, SOD activity decreased. This is consistent with Erman's findings that SOD activity under high temperature stress showed a trend of increasing and then decreasing [44]. This is because, as the stress temperature increases and the duration of stress prolongs, plants continue to increase the production of antioxidant enzymes within their own bodies. However, there comes a point where the plants' internal regulation cannot adapt quickly enough to the changing external environment, leading to a gradual decrease in antioxidant enzyme levels. Previous studies have reported that under various abiotic stresses, the production of reactive oxygen species (ROS) exceeds the cell's antioxidant defense capability, resulting in cellular damage [36].

In this study, we observed a notable increase in CAT activity during the first day of the HT and IL stress treatment. This finding aligns with previous research, suggesting that ginger plants activate the CAT pathway in response to stress, similar to rice (*Oryza sativa* L.), which demonstrates a prolonged elevation in CAT activity under HT stress [45]. Liebthal et al., however, reported a decrease in CAT activity in tomato leaves subjected to heat stress [46]. This discrepancy could be attributed to different sensitivity between plant species and diversity in growth conditions that lead to different responses. Comprehensive genomic analyses of the CAT family have been widely conducted and three CAT genes have been identified in *Arabidopsis* [47], maize [48], rice [49], and cucumber [50], while we identified four ginger CAT genes. The CAT genes (*CAT1-3*) in *Arabidopsis* showed differential expression under salt, cold, heat, and IL stress, but *CAT2* was mainly upregulated, while *CAT3* tended to be downregulated. *CAT2* was the gene with the most significant upregulation under IL; expression also significantly increased under heat stress [41]. In this study, CAT genes were all affected by HT and IL stress. Overall, the *ZoCAT1*, *ZoCAT3*, and *ZoCAT4* genes showed upregulation, with some variability in expression patterns under HT and IL stress. This suggests that these genes were involved in activating ROS metabolism. The expression of *ZoCAT2* gene was significantly downregulated, possibly due to some transcription factors inhibiting the expression of *ZoCAT2* gene. Similar reports have been found in *Arabidopsis*, in which transcription factor *WRKY75* inhibited the expression level of *AtCAT2*, enhanced ROS accumulation, and led to the senescence of *Arabidopsis* leaves [51].

Our results showed that LOX activity decreased gradually over time, suggesting a redirection of the plant's response pathway in coping with environmental stresses. This is consistent with earlier findings, where changes in LOX activity have been reported in other plant species, such as *Arabidopsis thaliana* [52]. The lower LOX activity may imply that the plant is mitigating the effects of the stress using an alternate pathway rather than the LOX-dependent pathway. Six types of LOX have been identified in *Arabidopsis* [53] and *AtLOX2* is required for wound-inducible JA accumulation, but it is unclear if it participates in responses to other stresses [54]. It has been reported that 13-LOX enzymes contribute to responses to abiotic stresses [50,55]. According to phylogenetic analysis, we found that ginger *ZoLOX* genes can also be divided into two subfamilies: 13-LOX and 9-LOX. The expression of the *ZoLOX18* gene belonging to the 13-LOX subfamily, which is close to *AtLOX2*, was significantly upregulated on the first day. Therefore, it is reasonable to speculate that *ZoLOX18* may also respond to HT and IL stress by affecting the JA biosynthesis pathway.

As nitrate is the substrate for the NR reduction process, it directly induces NR activity. NR catalyzes the formation of NO from nitrate or nitrite and NADH or NADPH [56]. NO generated through NR has been identified in sunflower (*Helianthus annuus* L.), spinach (*Spinacia oleracea* L.), and maize [56,57]. Low concentrations of NO and H₂O₂ act protectively in the defense response, but high concentrations of NO and H₂O₂ can cause serious damage to plant tissues [58,59]. NR activity decreased over time and exhibited a significant

reduction in NR activity on the third day of the HT and IL stress treatment. We also found that under IL stress, NR gene expression significantly changed and began to rise, reaching its peak on the second day, suggesting a negative effect of at least one of HT and IL on nitrogen assimilation. Ginger plantlets did not receive water during the 4-day exposure to the HT and IL environment. The effects of water deficiency cannot be excluded, although it would not cause death in ginger. It will be interesting to investigate the response of ginger to extreme drought in the future.

5. Conclusions

Ginger is sensitive to HT and IL stress, as evidenced by the decrease in chlorophyll index and the increase in MDA content. The present study provides new insights into the antioxidant responses of ginger plants to HT and IL stress. The results suggest that ginger plants activate multiple stress response pathways, including the SOD and CAT antioxidant defense mechanisms, and adjust their response over time by switching to different pathways. Furthermore, we found that the expression levels of genes involved in various stress response pathways, such as SOD, CAT, LOX, and NR, were differentially regulated under stress conditions. Our findings highlight the multifaceted nature of ginger plant responses to environmental stress and provide basic information for understanding the antioxidative protection mechanisms of the ginger plant.

Author Contributions: H.-L.L. and R.S. conceived the study; M.G., D.J., R.L., S.T. and H.X. performed the experiments; H.-L.L., M.G. and D.J. analyzed the data; H.-L.L., M.G., D.J., R.L., S.T., H.X., Z.C. and R.S. contributed reagents/materials/analysis tools; H.-L.L., M.G. and R.S. wrote the paper; H.-L.L. and R.S. edited the paper. All authors have read and agreed to the published version of the manuscript.

Funding: This research was funded by the Scientific and Technological Research Program of Chongqing Municipal Education Commission (KJZD-M202101301), Chongqing Science and Technology support projects (CSTB2022NSCQ-MSX1263), and Chongqing condiment industry system major special projects, Grant/Award Number: CQMAITS2023007.

Institutional Review Board Statement: Not applicable.

Informed Consent Statement: Not applicable.

Data Availability Statement: The datasets presented in this study are available upon request to the corresponding author. Data is not publicly available due to privacy.

Conflicts of Interest: Ran Liu is an employee of Chongqing Tianyuan Agricultural Technology Co., Ltd., Chongqing, China. The paper reflects the views of the scientists and not the company.

References

1. Gomez-Zavaglia, A.; Mejuto, J.C.; Simal-Gandara, J. Mitigation of emerging implications of climate change on food production systems. *Food Res. Int.* **2020**, *134*, 109256. [[CrossRef](#)] [[PubMed](#)]
2. Franco, J.; Bañón, S.; Vicente, M.; Miralles, J.; Martínez-Sánchez, J. Root development in horticultural plants grown under abiotic stress conditions—a review. *J. Hort. Sci. Biotechnol.* **2011**, *86*, 543–556. [[CrossRef](#)]
3. Castoria, R.; Caputo, L.; De Curtis, F.; De Cicco, V. Resistance of postharvest biocontrol yeasts to oxidative stress: A possible new mechanism of action. *Phytopathology* **2003**, *93*, 564–572. [[CrossRef](#)] [[PubMed](#)]
4. Rivero, R.M.; Mittler, R.; Blumwald, E.; Zandalinas, S.I. Developing climate-resilient crops: Improving plant tolerance to stress combination. *Plant J.* **2022**, *109*, 373–389. [[CrossRef](#)]
5. Pillai, S.; Oresajo, C.; Hayward, J. Ultraviolet radiation and skin aging: Roles of reactive oxygen species, inflammation and protease activation, and strategies for prevention of inflammation-induced matrix degradation—A review. *Int. J. Cosmet. Sci.* **2005**, *27*, 17–34. [[CrossRef](#)]
6. Sharma, P.; Jha, A.B.; Dubey, R.S.; Pessarakli, M. Reactive oxygen species, oxidative damage, and antioxidative defense mechanism in plants under stressful conditions. *J. Bot.* **2012**, *2012*, 217037. [[CrossRef](#)]
7. Ippolito, A.; Nigro, F. Impact of preharvest application of biological control agents on postharvest diseases of fresh fruits and vegetables. *Crop Prot.* **2000**, *19*, 715–723. [[CrossRef](#)]
8. Kong, F.; Ran, Z.; Zhang, J.; Zhang, M.; Wu, K.; Zhang, R.; Liao, K.; Cao, J.; Zhang, L.; Xu, J. Synergistic effects of temperature and light intensity on growth and physiological performance in *Chaetoceros calcitrans*. *Aquac. Rep.* **2021**, *21*, 100805. [[CrossRef](#)]

9. Lamaoui, M.; Jemo, M.; Datla, R.; Bekkaoui, F. Heat and drought stresses in crops and approaches for their mitigation. *Front. Chem.* **2018**, *6*, 26. [[CrossRef](#)]
10. Ozfidan-Konakci, C.; Yildiztugay, E.; Cavusoglu, H.; Arikan, B.; Elbasan, F.; Kucukoduk, M.; Turkan, I. Influences of sulfonated graphene oxide on gas exchange performance, antioxidant systems and redox states of ascorbate and glutathione in nitrate and/or ammonium stressed-wheat (*Triticum aestivum* L.). *Environ. Sci. Nano* **2021**, *8*, 3343–3364. [[CrossRef](#)]
11. Meitha, K.; Pramesti, Y.; Suhandono, S. Reactive oxygen species and antioxidants in postharvest vegetables and fruits. *Int. J. Food Sci.* **2020**, *2020*, 8817778. [[CrossRef](#)] [[PubMed](#)]
12. Karuppanapandian, T.; Moon, J.-C.; Kim, C.; Manoharan, K.; Kim, W. Reactive oxygen species in plants: Their generation, signal transduction, and scavenging mechanisms. *Aust. J. Crop Sci.* **2011**, *5*, 709–725.
13. Shu-Hsien, H.; Chih-Wen, Y.; Lin, C.H. Hydrogen peroxide functions as a stress signal in plants. *Bot. Bull. Acad. Sin.* **2005**, *46*, 1–10.
14. Bahuguna, R.N.; Jha, J.; Pal, M.; Shah, D.; Lawas, L.M.; Khetarpal, S.; Jagadish, K.S. Physiological and biochemical characterization of NERICA-L-44: A novel source of heat tolerance at the vegetative and reproductive stages in rice. *Physiol. Plant.* **2015**, *154*, 543–559. [[CrossRef](#)] [[PubMed](#)]
15. Porta, H.; Rocha-Sosa, M. Plant lipoxygenases. Physiological and molecular features. *Plant Physiol.* **2002**, *130*, 15–21. [[CrossRef](#)]
16. Fu, Y.-F.; Zhang, Z.-W.; Yang, X.-Y.; Wang, C.-Q.; Lan, T.; Tang, X.-Y.; Chen, G.-D.; Zeng, J.; Yuan, S. Nitrate reductase is a key enzyme responsible for nitrogen-regulated auxin accumulation in Arabidopsis roots. *Biochem. Biophys. Res. Commun.* **2020**, *532*, 633–639. [[CrossRef](#)]
17. Mittler, R.; Zandalinas, S.I.; Fichman, Y.; Van Breusegem, F. Reactive oxygen species signalling in plant stress responses. *Nat. Rev. Mol. Cell Biol.* **2022**, *23*, 663–679. [[CrossRef](#)]
18. Zhang, Y.; Luan, Q.; Jiang, J.; Li, Y. Prediction and utilization of malondialdehyde in exotic pine under drought stress using near-infrared spectroscopy. *Front. Plant Sci.* **2021**, *12*, 735275. [[CrossRef](#)]
19. Xu, Y.; Chu, C.; Yao, S. The impact of high-temperature stress on rice: Challenges and solutions. *Crop J.* **2021**, *9*, 963–976. [[CrossRef](#)]
20. Llorente, F.; López-Cobollo, R.M.; Catalá, R.; Martínez-Zapater, J.M.; Salinas, J. A novel cold-inducible gene from Arabidopsis, *RCI3*, encodes a peroxidase that constitutes a component for stress tolerance. *Plant J.* **2002**, *32*, 13–24. [[CrossRef](#)]
21. Zhang, B.; Chen, K.; Bowen, J.; Allan, A.; Espley, R.; Karunairetnam, S.; Ferguson, I. Differential expression within the LOX gene family in ripening kiwifruit. *J. Exp. Bot.* **2006**, *57*, 3825–3836. [[CrossRef](#)] [[PubMed](#)]
22. Upadhyay, R.K.; Handa, A.K.; Mattoo, A.K. Transcript abundance patterns of 9- and 13-lipoxygenase subfamily gene members in response to abiotic stresses (heat, cold, drought or salt) in tomato (*Solanum lycopersicum* L.) highlights member-specific dynamics relevant to each stress. *Genes* **2019**, *10*, 683. [[CrossRef](#)] [[PubMed](#)]
23. Jayaraman, A.; Puranik, S.; Rai, N.K.; Vidapu, S.; Sahu, P.P.; Lata, C.; Prasad, M. cDNA-AFLP analysis reveals differential gene expression in response to salt stress in foxtail millet (*Setaria italica* L.). *Mol. Biotechnol.* **2008**, *40*, 241–251. [[CrossRef](#)]
24. Curtis, I.; Power, J.; De Laat, A.; Caboche, M.; Davey, M. Expression of a chimeric nitrate reductase gene in transgenic lettuce reduces nitrate in leaves. *Plant Cell Rep.* **1999**, *18*, 889–896. [[CrossRef](#)]
25. Semwal, R.B.; Semwal, D.K.; Combrinck, S.; Viljoen, A.M. Gingerols and shogaols: Important nutraceutical principles from ginger. *Phytochemistry* **2015**, *117*, 554–568. [[CrossRef](#)]
26. Wang, Z.Q.; Wang, X.L.; Pu, Q.L. Analysis of meteorological conditions for high quality and high yield of Laiwu ginger. *Meteor. Mon.* **2006**, *12*, 102–106. (In Chinese)
27. Wang, Q.Z.; Fan, Y.Q.; Xu, F.X. The temperature suitability of Laiwu ginger. *J. Agric.* **2020**, *10*, 38–42. (In Chinese)
28. Jiang, S.G.; Xu, D.S.; Wu, Y.X.; Liu, M.Q. Impacts of Meteorological Conditions on Ginger Production and High-Yield Measures in Dabie Mountain Area. *Meteor. Sci. Technol.* **2011**, *39*, 106–109. (In Chinese)
29. Cao, X.Z.; Liu, L.; Zhang, K.Y.; Sun, L.H. Analysis of meteorological conditions during the growing period of ginger in Funing District, Qinhuangdao City, China. *Mod. Agric. Sci. Technol.* **2019**, *09*, 67–68. (In Chinese)
30. Li, H.L.; Huang, M.J.; Tan, D.Q.; Liao, Q.H.; Zou, Y.; Jiang, Y.S. Effects of soil moisture content on the growth and physiological status of ginger (*Zingiber officinale* Roscoe). *Acta Physiol. Plant.* **2018**, *40*, 125. [[CrossRef](#)]
31. Senthilkumar, M.; Amaresan, N.; Sankaranarayanan, A.; Senthilkumar, M.; Amaresan, N.; Sankaranarayanan, A. Estimation of malondialdehyde (MDA) by thiobarbituric acid (TBA) assay. In *Plant-Microbe Interactions*; Springer: New York, NY, USA, 2021.
32. Shi, G.; Zhu, X. Genome-wide identification and functional characterization of CDPK gene family reveal their involvement in response to drought stress in *Gossypium barbadense*. *PeerJ* **2022**, *10*, e12883. [[CrossRef](#)]
33. Kumar, S.; Stecher, G.; Tamura, K. MEGA7: Molecular evolutionary genetics analysis version 7.0 for bigger datasets. *Mol. Biol. Evol.* **2016**, *33*, 1870–1874. [[CrossRef](#)]
34. Livak, K.J.; Schmittgen, T.D. Analysis of relative gene expression data using real-time quantitative PCR and the $2^{-\Delta\Delta CT}$ method. *Methods* **2001**, *25*, 402–408. [[CrossRef](#)]
35. Qu, X.; Wang, H.; Chen, M.; Liao, J.; Yuan, J.; Niu, G. Drought stress-induced physiological and metabolic changes in leaves of two oil tea cultivars. *J. Am. Soc. Hortic. Sci.* **2019**, *144*, 439–447. [[CrossRef](#)]
36. Almeselmani, M.; Deshmukh, P.S.; Sairam, R.K.; Kushwaha, S.R.; Singh, T.P. Protective role of antioxidant enzymes under high temperature stress. *Plant Sci.* **2006**, *171*, 382–388. [[CrossRef](#)]
37. Berwal, M.; Ram, C. Superoxide dismutase: A stable biochemical marker for abiotic stress tolerance in higher plants. In *Abiotic and Biotic Stress in Plants*; Intech Open: London, UK, 2018; pp. 1–10.

38. Aleem, M.; Aleem, S.; Sharif, I.; Wu, Z.; Aleem, M.; Tahir, A.; Atif, R.M.; Cheema, H.M.N.; Shakeel, A.; Lei, S. Characterization of SOD and GPX gene families in the soybeans in response to drought and salinity stresses. *Antioxidants* **2022**, *11*, 460. [[CrossRef](#)]
39. Manivannan, P.; Jaleel, C.A.; Sankar, B.; Kishorekumar, A.; Somasundaram, R.; Lakshmanan, G.A.; Panneerselvam, R. Growth, biochemical modifications and proline metabolism in *Helianthus annuus* L. as induced by drought stress. *Colloids Surf. B* **2007**, *59*, 141–149. [[CrossRef](#)]
40. Fahad, S.; Bajwa, A.A.; Nazir, U.; Anjum, S.A.; Farooq, A.; Zohaib, A.; Sadia, S.; Nasim, W.; Adkins, S.; Saud, S. Crop production under drought and heat stress: Plant responses and management options. *Front. Plant Sci.* **2017**, *8*, 1147. [[CrossRef](#)]
41. Filiz, E.; Ozyigit, I.I.; Saracoglu, I.A.; Uras, M.E.; Sen, U.; Yalcin, B. Abiotic stress-induced regulation of antioxidant genes in different Arabidopsis ecotypes: Microarray data evaluation. *Biotechnol. Biotechnol. Equip.* **2019**, *33*, 128–143. [[CrossRef](#)]
42. Hu, W.; Zhang, J.; Yan, K.; Zhou, Z.; Zhao, W.; Zhang, X.; Pu, Y.; Yu, R. Beneficial effects of abscisic acid and melatonin in overcoming drought stress in cotton (*Gossypium hirsutum* L.). *Physiol. Plant.* **2021**, *173*, 2041–2054. [[CrossRef](#)]
43. Baek, K.-H.; Skinner, D.Z. Alteration of antioxidant enzyme gene expression during cold acclimation of near-isogenic wheat lines. *Plant Sci.* **2003**, *165*, 1221–1227. [[CrossRef](#)]
44. Hong, E.; Xia, X.Z.; Ji, W.; Li, T.Y.; Xu, X.Y.; Chen, J.R.; Chen, X.; Zhu, X.T. Effects of High Temperature Stress on the Physiological and Biochemical Characteristics of *Paeonia ostia*. *Int. J. Mol. Sci.* **2023**, *24*, 11180. [[CrossRef](#)]
45. Das, K.; Roychoudhury, A. Reactive oxygen species (ROS) and response of antioxidants as ROS-scavengers during environmental stress in plants. *Front. Environ. Sci.* **2014**, *2*, 53. [[CrossRef](#)]
46. Wang, J.; Xu, J.; Wang, L.; Zhou, M.; Nian, J.; Chen, M.; Lu, X.; Liu, X.; Wang, Z.; Cen, J. SEMI-ROLLED LEAF 10 stabilizes catalase isozyme B to regulate leaf morphology and thermotolerance in rice (*Oryza sativa* L.). *Plant Biotechnol. J.* **2023**, *21*, 819–838. [[CrossRef](#)]
47. McClung, C.R. Regulation of catalases in Arabidopsis. *Free Radic. Biol. Med.* **1997**, *23*, 489–496. [[CrossRef](#)]
48. Sytykiewicz, H. Transcriptional responses of *catalase* genes in maize seedlings exposed to cereal aphids' herbivory. *Biochem. Syst. Ecol.* **2015**, *60*, 131–142. [[CrossRef](#)]
49. Joo, J.; Lee, Y.H.; Song, S.I. Rice *CatA*, *CatB*, and *CatC* are involved in environmental stress response, root growth, and photorespiration, respectively. *J. Plant Biol.* **2014**, *57*, 375–382. [[CrossRef](#)]
50. Hu, L.; Yang, Y.; Jiang, L.; Liu, S. The *catalase* gene family in cucumber: Genome-wide identification and organization. *Genet. Mol. Res.* **2016**, *39*, 408–415. [[CrossRef](#)]
51. Guo, P.; Li, Z.; Huang, P.; Li, B.; Fang, S.; Chu, J.; Guo, H. A tripartite amplification loop involving the transcription factor WRKY75, salicylic acid, and reactive oxygen species accelerates leaf senescence. *Plant Cell* **2017**, *29*, 2854–2870. [[CrossRef](#)]
52. Koo, A.J.; Cooke, T.F.; Howe, G.A. Cytochrome P450 CYP94B3 mediates catabolism and inactivation of the plant hormone jasmonoyl-L-isoleucine. *Proc. Natl. Acad. Sci. USA* **2011**, *108*, 9298–9303. [[CrossRef](#)]
53. Browse, J. Jasmonate passes muster: A receptor and targets for the defense hormone. *Annu. Rev. Plant Biol.* **2009**, *60*, 183–205. [[CrossRef](#)]
54. de la Haba, P.; Agüera, E.; Benítez, L.; Maldonado, J.M. Modulation of nitrate reductase activity in cucumber (*Cucumis sativus*) roots. *Plant Sci.* **2001**, *161*, 231–237. [[CrossRef](#)]
55. ul Hassan, M.N.; Zainal, Z.; Ismail, I. Green leaf volatiles: Biosynthesis, biological functions and their applications in biotechnology. *Plant Biotechnol. J.* **2015**, *13*, 727–739. [[CrossRef](#)]
56. Rockel, P.; Strube, F.; Rockel, A.; Wildt, J.; Kaiser, W.M. Regulation of nitric oxide (NO) production by plant nitrate reductase in vivo and in vitro. *J. Exp. Bot.* **2002**, *53*, 103–110. [[CrossRef](#)]
57. Yamasaki, H.; Sakihama, Y. Simultaneous production of nitric oxide and peroxyxynitrite by plant nitrate reductase: In vitro evidence for the NR-dependent formation of active nitrogen species. *FEBS Lett.* **2000**, *468*, 89–92. [[CrossRef](#)]
58. Beligni, M.V.; Lamattina, L. Nitric oxide counteracts cytotoxic processes mediated by reactive oxygen species in plant tissues. *Planta* **1999**, *208*, 337–344. [[CrossRef](#)]
59. Delledonne, M.; Murgia, I.; Ederle, D.; Sbicego, P.F.; Biondani, A.; Polverari, A.; Lamb, C. Reactive oxygen intermediates modulate nitric oxide signaling in the plant hypersensitive disease-resistance response. *Plant Physiol. Biochem.* **2002**, *40*, 605–610. [[CrossRef](#)]

Disclaimer/Publisher's Note: The statements, opinions and data contained in all publications are solely those of the individual author(s) and contributor(s) and not of MDPI and/or the editor(s). MDPI and/or the editor(s) disclaim responsibility for any injury to people or property resulting from any ideas, methods, instructions or products referred to in the content.